

MIMO CAPACITY IN UWB CHANNELS IN AN OFFICE ENVIRONMENT FOR DIFFERENT POLARIZATIONS

Concepcion Garcia-Pardo*, Jose-Maria Molina-Garcia-Pardo, José-Víctor Rodríguez, and Leandro Juan Llacer

Information Technologies and Communications Department, Technical University of Cartagena, Plaza del Hospital, 1 Antiguo Cuartel de Antigones, Cartagena 30202, Spain

Abstract—In this paper, a 4×4 indoor Multiple-Input Multiple-Output Ultra-Wideband (MIMO-UWB) measurement campaign in the 2–5 GHz bandwidth is presented. The main contribution of this work is the impact of radio-wave polarization as well as the effect of frequency dependence on the capacity of MIMO-UWB systems working in an office environment. To accomplish this, the capacity for different polarizations is analyzed under two different assumptions: constant or variable Signal-to-Noise Ratio.

1. INTRODUCTION

Ultra-Wideband (UWB) signals are defined as those whose bandwidth is larger than 500 MHz and/or larger than 20% of the central frequency [1]. UWB communications have gained the interest of the research community thanks to its high precision and low transmitted power given rise to many applications such as Body Area Networks (BAN) [2]. However, the regulatory bodies in the United States and Europe have strongly restricted the transmitted power of these systems due to their interference with existent communication systems. These restrictions make necessary a thorough study of the propagation channel in order to achieve the best performance of future UWB devices.

Multiple-Input Multiple-Output (MIMO) systems are considered one of the best techniques to optimize the use of the transmission spectrum and power [3, 4]. This technique benefits from the use of multiple n -dimensional antennas [5] at both sides of the radio interface,

Received 3 June 2013, Accepted 22 September 2013, Scheduled 24 September 2013

* Corresponding author: Concepcion Garcia-Pardo (conchi.gpardo@upct.es).

so that by using a proper space-time code, either the diversity and/or the throughput can be substantially improved [6]. Furthermore, it has been shown that the use of polarization for spatial multiplexing-based MIMO systems can lead to significant performance improvements, and consequently many researchers have addressed the polarization multiplexing/diversity issue. Indoor channel measurements with dual-polarized or hybrid array configurations have been reported in the literature [7–9].

The use of MIMO in UWB systems has been addressed as one possible solution to improve the UWB link robustness or its range [10] as well as the error-rate considerably [11–13]. In [14, 15] some results on the channel capacity of UWB-MIMO systems are presented. Furthermore, in [16] it was found that polarization diversity is sometimes more effective than temporal multipath diversity, so the required number of rake fingers can be reduced. However, although polarization has been widely analyzed for conventional MIMO systems [17–20], there is not much information in the scientific literature about the effect of polarization in MIMO-UWB systems.

In this paper, we report the results of a 4×4 MIMO-UWB indoor measurement campaign in the 2–5 GHz band performed at the laboratories of the underground level of one of the buildings of the Technical University of Cartagena. Single antenna parameters as well as multiantenna characteristics are analyzed. The work presented here also presents a comparison with the results obtained for 200 MHz bandwidth [21], so therefore the channel sounder, antenna arrays and the environment are the same. Therefore, the effect of the increment of the bandwidth (from 200 MHz to 3 GHz) is also taken into account.

This paper is organized as follows: Section 2 describes the environment, the MIMO-UWB channel sounding procedure, and the data analysis. Sections 3 and 4 focus on the capacity for constant and variable signal-to-noise ratio (SNR). Finally, Section 5 concludes the findings of this paper.

2. CHANNEL SOUNDING AND DATA ANALYSIS

2.1. Description of the Environment

The measurement campaign was carried out in the underground level of the Technical University of Cartagena. It mainly consists of a 50 m long corridor, three perpendicular corridors, and some labs. A photo of the environment is shown in Fig. 1 and a top view of the selected indoor environment is depicted in Fig. 2. The walls of this building are made of plasterboard; the floor is made of reinforced concrete, and so is the ceiling.



Figure 1. Photo of the main corridor and laboratories where measurement campaign took place.

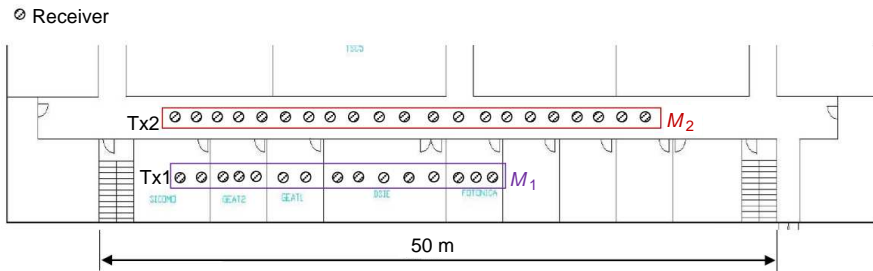


Figure 2. Floor plan of the measurement environment.

2.2. Channel Sounder Setup

The MIMO-channel sounder used to perform the measurements is based on a multiport network analyzer (MNA) and a fast switch. The receiving antennas are directly connected to the ports of the MNA. One port of the MNA is configured as a transmitter and connected to an optical link (RF/OF and OF/RF), which carries the signal to the fast switch. Finally, the transmitting antennas are connected to the fast switch, so that the signal from the optical link is transmitted sequentially to each element of the transmitter array. All the measurement procedure is controlled by a laptop as shown in Fig. 3.

For the UWB measurements, we have used eight Electro-

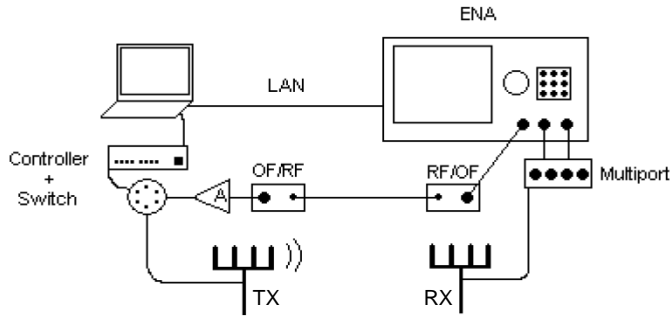


Figure 3. Block diagram of the MIMO channel sounder.



(a)



(b)

Figure 4. Photo of (a) the antenna used in the experiments and (b) the array installed in the mast.

Metrics omnidirectional mast-mounted antennas (EM-6116), as can be observed in Fig. 4. These antennas work in the 2–10 GHz frequency band and have been widely used in literature for UWB measurements [22–25] since they operate in the UWB band. Furthermore, the antennas have 1 dBi gain and an XPD of 12 dB.

The power transmitted by each antenna was -13 dBm and the noise was -108 dBm, so the dynamic range of the channel sounder was greater than 90 dB, which was enough to assure a high SNR for most of the measurements.

Due to the limitations of the optical link the maximum frequency that can be measured is 5 GHz. Thus, the channel was sounded from $f_{\min} = 2$ to $f_{\max} = 5$ GHz by measuring 801 frequency points over the

$BW = 3$ GHz bandwidth. Therefore, the resulting frequency resolution is $\Delta f = 3.75$ MHz.

The transmitter is located in two different positions (Tx1, in the middle of one laboratory, and Tx2 in the corridor) and the receivers have been classified into three groups: M_1 , where the receiver moves across five small consecutive labs (LoS and NLoS situations with Tx1), and M_2 , where the receiver moves along the main corridor (LoS with Tx2).

Furthermore, for each position of M_1 , four configurations of the arrays have been measured. If we define V as vertical polarization and H as horizontal polarization for the elements of the array, the mentioned four combinations are VV and HH (also called copolar polarizations) and HV and VH (also called crosspolar polarizations), as can be seen in Fig. 5, in which the first letter refers to the transmitter and the second to the receiver. Each array is linear and uniformly spaced due to the fact that although it has been reported in literature better performances for non-uniform and non-linear arrays [26–29], the aim of this measurement campaign was to compare the results obtained with those deduced in [21] for 200 MHz bandwidth. The large size of the antennas made us to separate the elements of the array at least 4 cm. Therefore, the antenna spacing had to be set to $2\lambda = 6$ cm (with λ referred to the maximum frequency), although smaller spacings can provide higher performances of the MIMO link [28, 29].

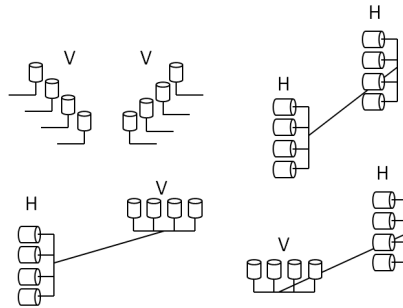


Figure 5. Different polarizations for the arrays.

Summarizing, corresponding to each position of the receiver on the route and each polarization we define the MIMO frequency domain transfer function, $\mathbf{G}(n, m, f, t)$, where n denotes the receiving element of the array, m the transmitting element of the array, f the frequency point within the measured bandwidth, and t the snapshot. We have used $n = 4$ receiving elements, $m = 4$ transmitting elements, and $f = 801$ frequency points. The stationarity of the channel is assured

by taking $t = 5$ snapshots of each measurement, which also improves the SNR of the measurements. Thus, for each position and polarization \mathbf{G} is a matrix of dimensions $4 \times 4 \times 801 \times 5$.

2.3. Data Analysis

We analyze the capacity for the $M \times N$ MIMO system that can be obtained from the \mathbf{G} matrices as [6]:

$$C = \log_2 \left(\det \left(\mathbf{I}_N + \frac{\text{SNR}}{M} \mathbf{H}\mathbf{H}^\dagger \right) \right) \text{ bit/s/Hz} \quad (1)$$

where \mathbf{I}_N is the $N \times N$ identity matrix, \dagger represents the conjugate transpose operation, \mathbf{H} is the Frobenius normalized \mathbf{G} matrix, and SNR is the Signal-to-Noise Ratio at the receiver. Uniform linear arrays having four elements ($M = N = 4$) have been considered. The capacity over the 3 GHz bandwidth has been averaged for each case. Furthermore, all \mathbf{G} matrices having at least one element with a measured SNR of 10 dB or less have been discarded. Therefore, a SNR higher than 10 dB is guaranteed so the noise does not mask the results. The correlation coefficient at each frequency between a pair of antennas of the array is computed as in [30].

With regard to SNR in (1), two cases can be considered. On the one hand, MIMO capacity can be studied by assuming a constant received power. For example, we can consider a receiver which adjusts the received power using an automatic gain control (AGC) amplifier. This results in a constant SNR available in all positions of the receiver independently of the received power, and the effect of spatial richness is directly observed in the capacity curves. On the other hand, one can think of a system where the transmitted power is fixed and the SNR at the receiver is determined mainly by the path loss. In this case, capacity shows effects related to both the received power and the spatial richness. Consequently, the study of capacity in different environments has been divided into two cases: constant received power and constant transmitted power. The results are presented in the following sections.

3. CAPACITY FOR CONSTANT RECEIVED POWER

3.1. Capacity along the Corridor in LoS

Firstly, we will study the capacity performance in a corridor environment for the group of measurements M_2 in LoS. To accomplish this, we have chosen some significant positions of the receiver: two before the T junction, the third in the T junction, and the last one

at the end of the main corridor, that is, when the receiver is in the positions 1, 6, 13, and 21 of M_2 . The CCDF (Complementary Cumulative Distribution Function) of the normalized capacity (for an SNR of 10 dB) for all polarizations has been computed and results are summarized in Table 1 for a probability of 90%.

Table 1. Correlations, and capacity for SNR fixed at 10 dB when probability > 0.9 in corridor scenario.

		Tx Correlation	Rx Correlation	Capacity (90%)
Rx1 $d_{TX-RX} = 2\text{ m}$	<i>HH</i>	0.55	0.56	8.9
	<i>VV</i>	0.49	0.49	9.7
	<i>HV</i>	0.54	0.54	9.4
	<i>VH</i>	0.56	0.55	9.1
Rx6 $d_{TX-RX} = 12\text{ m}$	<i>HH</i>	0.48	0.48	10.1
	<i>VV</i>	0.47	0.47	10.0
	<i>HV</i>	0.50	0.49	9.8
	<i>VH</i>	0.51	0.51	9.6
Rx3 $d_{TX-RX} = 26\text{ m}$ (<i>T</i> Junction)	<i>HH</i>	0.45	0.46	10.1
	<i>VV</i>	0.48	0.48	10.2
	<i>HV</i>	0.52	0.52	9.4
	<i>VH</i>	0.48	0.48	9.8
Rx21 $d_{TX-RX} = 40\text{ m}$	<i>HH</i>	0.49	0.50	9.6
	<i>VV</i>	0.52	0.52	9.6
	<i>HV</i>	0.52	0.52	9.2
	<i>VH</i>	0.52	0.52	9.3

In this scenario, the copolar configurations outperform the crosspolar ones. The same effect was observed in LoS for 200 MHz bandwidth [21]. The highest capacity is provided in the position next to the *T* junction (position 3, Rx3 = 26 m), where the lowest correlation coefficient is also given. This behavior is a consequence of the multiple reflections coming from the corridor on the left.

Furthermore, the capacity for *HH*, *VV*, *HV*, and *VH* at the end of the corridor tends to converge due to a depolarization of the radio waves along the corridor [31].

3.2. Capacity across the Laboratories

Next, the capacity for constant received power in the laboratories' conditions will be studied by analyzing the group of measurements M_1 .

Table 2. Correlations, and capacity for SNR fixed at 10 dB when probability > 0.9 in corridor scenario.

		Tx Correlation	Rx Correlation	Capacity (90%)
Room 1	<i>HH</i>	0.55	0.56	9.1
	<i>VV</i>	0.56	0.57	9.1
	<i>HV</i>	0.57	0.56	9.2
	<i>VH</i>	0.59	0.62	8.7
Room 2	<i>HH</i>	0.55	0.58	8.9
	<i>VV</i>	0.56	0.57	9.0
	<i>HV</i>	0.52	0.51	9.5
	<i>VH</i>	0.54	0.55	9.2
Room 3	<i>HH</i>	0.55	0.56	8.9
	<i>VV</i>	0.52	0.52	9.6
	<i>HV</i>	0.48	0.48	9.8
	<i>VH</i>	0.46	0.46	10.1

Again, the CCDFs of capacity in each laboratory (room) have been computed and the results are summarized in Table 2 for a probability of 90%. In Room 1 the receiver is in LoS with the transmitter, while in Rooms 2 and 3 the receiver is in NLoS.

It should be noted that after the second and third walls only some points of *HH* and *VV* polarizations meet the SNR requirements described in Subsection 2.3. Therefore, results for those points are not presented.

The way in which capacity increases with the number of walls penetrated can be observed. Thus, the highest values of capacity correspond to the furthest laboratory (room 3) for all polarizations. Consequently, this performance also corresponds to a decrease in the correlation coefficient with distance. Besides, the crosspolar polarizations present higher capacity than copolar ones, in contrast to the performance in LoS (M_2). This also agrees with the results provided in [21] for 200 MHz bandwidth, where in NLoS crosspolar polarizations outperform the copolar configuration.

4. CAPACITY FOR CONSTANT TRANSMITTED POWER

4.1. Capacity along the Corridor in LoS

Next, we will study the performance of the capacity in a corridor environment for the group of measurements M_2 in the case of constant transmitted power, that is, in the case of using the measured SNR

in the receiver. To fairly compare the performance of the capacity for the two groups of measurements, we have chosen a reference point corresponding to a SNR of 10 dB for the VV configuration at the end of the corridor (last position of M_2), where the lowest value of received power was found. An extra threshold of 10 dB above such a level was also added. The measured XPD in this environment is around 7.5 dB [31].

The way in which capacity decreases exponentially with distance as SNR does can be observed in Fig. 6. In this case, the effect of the SNR is much higher than that which comes from the correlation. Therefore, in this scenario, capacity is clearly higher for copolar polarizations although capacity for all configurations tends to converge at the end of the corridor due to the depolarization of the radio waves with distance [31].

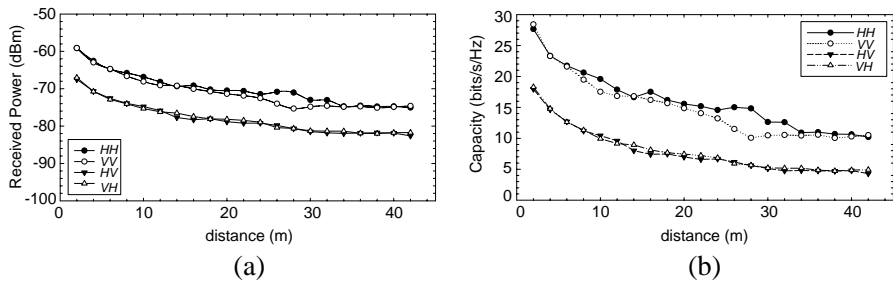


Figure 6. (a) Received power and (b) the measured capacity as a function of distance in the main corridor (M_2) in LoS, for a variable SNR.

4.2. Capacity across the Laboratories

Secondly, the capacity for constant transmitted power (SNR variable) will be analyzed. In this case, the variable SNR is referred to the measured SNR for VV polarization in the last room (just before wall 4). In Fig. 7 the capacity for the group of measurements M_1 is depicted. After the second and third walls only some points of HH and VV polarizations meet the SNR requirements, so results for those points are not presented.

Since SNR decreases in the same manner as path loss, capacity decreases with distance and exhibits strong decrements after each wall. Again, this performance of the capacity was observed for 200 MHz bandwidth in [21].

Furthermore, as in the corridor scenario, copolar configurations outperforms crosspolar ones due to the fact that the effect of the SNR

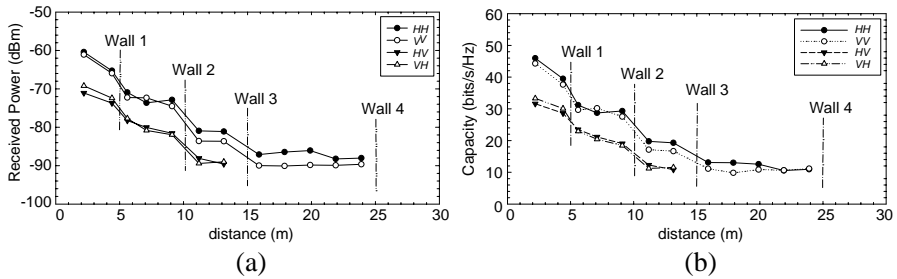


Figure 7. (a) Received power and (b) the measured capacity as a function of distance in the laboratories (M_1), for a variable SNR.

dominates over the effect of correlation, although the channel is highly decorrelated.

A similar behavior of the capacity was observed for 200 MHz bandwidth in [21].

5. CONCLUSION

In this paper, results from an indoor 4×4 MIMO-UWB measurement campaign in the 2–5 GHz band have been reported. The capacity of the 4×4 MIMO-UWB system was analyzed in different environments for different polarizations (HH , VV , HV , and VH) under two different hypotheses: the first one, in the case of constant received power (constant SNR) and the second one in the case of constant transmitted power (variable SNR).

In the case of constant SNR, the capacity for the copolar configurations (VV and HH polarizations) in LoS conditions was found to be higher than for the crosspolar ones. However, the contrary behavior was found when the receiver was in NLoS with the transmitter.

In the case of variable SNR, the capacity was strongly influenced by the SNR and the XPD. Thus, in this more realistic case, use a crosspolar configuration does not provide any improvement on the system capacity. Furthermore, the effect of SNR dominates over the effect of correlation due to the fact that although correlation is higher in NLoS for crosspolar configurations, the capacity is lower due to a lower SNR. Thus, copolar configuration would be the more suitable configuration in a real system.

Finally, it can be also remarked that the same behavior of the capacity was found in a similar analysis performed in [21] for 200 MHz bandwidth.

ACKNOWLEDGMENT

This work was supported by the Ministerio de Economía y Competitividad (MINECO), Spain (TEC2010-20841-C04-03) and by European FEDER funds.

REFERENCES

1. Molisch, A. F., "Ultra-wide-band propagation channels," *Proceedings of the IEEE*, Vol. 97, No. 2, 353–371, Feb. 2009.
2. Abouda, A. A., H. M. El-Sallabi, and S. G. Häggman, "Effect of antenna array geometry and ULA azimuthal orientation on MIMO channel properties in urban city street grid," *Progress In Electromagnetics Research*, Vol. 64, 257–278, 2006.
3. Winters, J., "On the capacity of radio communication systems with diversity in a Rayleigh fading environment," *IEEE Journal on Selected Areas in Communications*, Vol. 5, No. 5, 871–878, Jun. 1987.
4. Foschini, G. J. and M. J. Gans, "On limits of wireless communications in a fading environment when using multiple antennas," *Wireless Personal Commun.*, Vol. 6, No. 3, 311–335, Mar. 1998.
5. Di Bari, R., Q. H. Abbasi, A. Alomainy, and Y. Hao, "An advanced UWB channel model for body-centric wireless networks," *Progress In Electromagnetics Research*, Vol. 136, 79–99, 2013.
6. Gesbert, D., M. Shafi, D.-S. Shiu, P. Smith, and A. Naguib, "From theory to practice: An overview of MIMO space-time coded wireless systems," *IEEE Journal on Selected Areas in Communications*, Vol. 21, No. 3, 281–302, Apr. 2003.
7. Zhao, X., S. Geng, L. Vuokko, J. Kivinen, and P. Vainikainen, "Polarization behaviors at 2, 5 and 60 GHz for indoor mobile communications," *Wireless Personal Commun.*, Vol. 27, No. 2, 99–115, Nov. 2003.
8. Kyritsi, P., D. C. Cox, R. A. Valenzuela, and P. W. Wolniansky, "Effect of antenna polarization on the capacity of a multiple element system in an indoor environment," *IEEE Journal on Selected Areas in Communications*, Vol. 20, No. 6, 1227–1239, Aug. 2002.
9. Wallace, J. W., M. A. Jensen, and A. L. Swindlehurst, "Experimental characterization of the MIMO wireless channel:

- Data acquisition and analysis,” *IEEE Trans. Wireless Commun.*, Vol. 2, No. 2, 335–343, Mar. 2003.
10. Sibille, A., “Time-domain diversity in ultra-wideband MIMO communications,” *EURASIP Journal on Applied Signal Processing*, Vol. 3, 316–327, 2005
 11. Wang, L.-C., W.-C. Liu, and K.-J. Shieh, “On the performance of using multiple transmit and receive antennas in pulse-based ultrawideband systems,” *IEEE Trans. Wireless Commun.*, Vol. 4, No. 6, 2738–2750, Nov. 2005.
 12. Yang, L. and G. B. Giannakis, “Analog space-time coding for multiantenna ultra-wideband transmissions,” *IEEE Trans. Commun.*, Vol. 52, No. 3, 507–517, Mar. 2004.
 13. Liu, H., R. C. Qiu, and Z. Tian, “Error performance of pulse-based ultrawideband MIMO systems over indoor wireless channels,” *IEEE Trans. Wireless Commun.*, Vol. 4, No. 6, 2939–2944, Nov. 2005.
 14. Malik, W. Q. and D. J. Edwards, “Measured MIMO capacity and diversity gain with spatial and polar arrays in ultrawideband channels,” *IEEE Trans. Commun.*, Vol. 55, No. 12, 2361–2370, Dec. 2007.
 15. Zheng, F. and T. Kaiser, “On the evaluation of channel capacity of multi-antenna UWB indoor wireless systems,” *Proc. 2004 IEEE Int. Symp. Spread Spectrum Tech. Applicat.*, 525–529, Sydney, Australia, Aug. 30–Sep. 2, 2004.
 16. Zheng, F. and T. Kaiser, “On the evaluation of channel capacity of UWB indoor wireless systems,” *IEEE Trans. Signal Process.*, Vol. 56, No. 12, 6106–6113, 2008.
 17. Malik, W. Q. and D. J. Edwards, “Measured MIMO capacity and diversity gain with spatial and polar arrays in ultrawideband channels,” *IEEE Trans. Commun.*, Vol. 55, No. 12, 2361–2370, 2007.
 18. Erceg, V., P. Soma, D. S. Baum, and S. Catreux, “Multiple-input multiple-output fixed wireless radio channel measurements and modelling using dual-polarized antennas at 2.5 GHz,” *IEEE Trans. Wireless Commun.*, Vol. 3, No. 6, 2288–2298, Nov. 2004.
 19. Oestges, C., V. Erceg, and A. J. Paulraj, “Propagation modeling of MIMO multipolarized fixed wireless channels,” *IEEE Transactions on Vehicular Technology*, Vol. 53, No. 3, 644–654, May 2004.
 20. Quitin, F., C. Oestges, F. Horlin, and P. De Doncker, “Polarization measurements and modeling in indoor NLOS

- environments,” *IEEE Trans. Wireless Commun.*, Vol. 9, No. 1, 21–25, Jan. 2010.
21. Molina-Garcia-Pardo, J. M., J.-V. Rodríguez, and L. Juan-Llacer, “Polarized indoor MIMO channel measurements at 2.45 GHz,” *IEEE Transactions on Antennas and Propagation*, Vol. 56, No. 12, 3818–3828, 2008.
 22. Chehri, A., P. Fortier, and P. M. Tardif, “Large-scale fading and time dispersion parameters of UWB channel in underground mines,” *International Journal of Antennas and Propagation*, Vol. 2008, Article ID 806326, 10 Pages, 2008, DOI: 10.1155/2008/806326.
 23. Nkakanou, B., G. Y. Delisle, and N. Hakem, “Experimental characterization of ultra-wideband channel parameter measurements in an underground mine,” *Journal of Computer Networks and Communications*, Vol. 2011, Article ID 157596, 7 Pages, 2011, DOI: 10.1155/2011/157596.
 24. Ghaddar, M. and L. Talbi, “NLOS UWB undermining experimental characterization & performance evaluation using MB-OFDM,” *PIERS Proceedings*, 1530–1534, Marrakesh, Morocco, Mar. 20–23, 2011.
 25. Garcia-Pardo, C., J.-M. Molina-García-Pardo, M. Lienard, D. P. Gaillot, and P. Degauque, “Double directional channel measurements in an arched tunnel and interpretation using ray tracing in a rectangular tunnel,” *Progress In Electromagnetics Research M*, Vol. 22, 91–107, 2012.
 26. Recioui, A. and H. Bentarzi, “Genetic algorithm based MIMO capacity enhancement in spatially correlated channels including mutual coupling,” *Wireless Personal Commun.*, Vol. 63, No. 3, 689–701, Springer, 2012, DOI: 10.1007/s11277-010-0159-5.
 27. Recioui, A. and H. Bentarzi, “Capacity optimization of MIMO wireless communication systems using a hybrid genetic-Taguchi algorithm,” *Wireless Personal Commun.*, Vol. 71, No. 2, 2013, DOI: 10.1007/s11277-012-0857-2.
 28. Durrani, S. and M. E. Bialkowski, “An investigation into the interference rejection capability of a linear array in a wireless communications system,” *Microwave and Optical Technology Letters*, Vol. 35, No. 6, 445–449, Dec. 2002.
 29. Durrani, S. and M. E. Bialkowski, “Effect of mutual coupling on the interference rejection capabilities of linear and circular arrays in CDMA systems,” *IEEE Transactions on Antennas and Propagation*, Vol. 52, No. 4, 1130–1134, Apr. 2004.

30. Liénard, M., P. Degauque, J. Baudet, and D. Degardin, "Investigation on MIMO channels in subway tunnels," *IEEE Journal on Selected Areas in Communications*, Vol. 21, No. 3, 332–339, 2003.
31. Garcia-Pardo, C., J.-M. Molina-Garcia-Pardo, A. Garrido-Cervantes, J. D. Muhehe, and L. Juan-Llaser, "Frequency dependence of 2–5 GHz polarized UWB channel parameters in office environment," *IEEE Transactions on Antennas and Propagation*, Vol. 60, No. 6, 2970–2979, Jun. 2012.